Journal of Engineering Science and Technology
Vol. 13, No. 4 (2018) 943 - 963

EXPERIMENTAL STUDY ON WEAR OF MIXED CERAMIC TOOL AND CORRELATION ANALYSIS BETWEEN SURFACE ROUGHNESS AND CUTTING TOOL RADIAL VIBRATIONS DURING HARD TURNING OF AISI 52100 STEEL

YOUCEF ABIDI*, LAKHDAR BOULANOUAR, ABDELAZIZ AMIRAT

Advanced Technologies in Mechanical Production Research Laboratory (LRTAPM),
Badji Mokhtar - Annaba University, P.O Box 12, 23000 Annaba, Algeria
*Corresponding Author:youcef.abidi@alsolb-dz.com

Abstract

Wear investigation has been conducted on mixed ceramic cutting tool (70% Al_2O_3 + 30% TiC) when machining hardened AISI 52100 steel (66 HRC). Experimental planning method has been used to assess the relationship between radial cutting vibrations and surface roughness as a function of the machining conditions. First, wear results show that when the cutting speed is increased 3.78 times, tool life drops of 8.75 times. When increasing the feed rate by a factor of 2.75 tool life decreases by a factor of 1.4. Then, the effect of cutting parameters (speed, feed and depth) on one hand surface roughness (*Ra*) and in the other hand radial tool vibrations has been determined using the multiple regression models with a coefficient of determination R^2 equal to respectively 95.5% and 89.3%. With regards to surface roughness, ANOVA analyses reveal that feed rate contributes of about 84% in the surface roughness. Meanwhile, looking at the vibration phenomena, the cutting speed has the most significant effect on the values of radial tool vibrations comparing to depth and feed rate effect. Finally the correlation between surface roughness and tool radial vibrations has been analyzed through the linear and nonlinear correlation coefficients. The values of Pearson and Spearman coefficient were respectively low 0.465 and 0.554 showing that above 1000 rpm of cutting speed, the machining system is no more stable generating a great effect of cutting vibrations.

Keywords: Hard machining, Wear, Lifetime, Mixed ceramic tool, Surface roughness, Tool vibration, ANOVA.

1. Introduction

Hard turning is nowadays, considered as a chip removal manufacturing process

Nomenclature

a	Depth of cut, mm
f	Feed rate, mm/rev
R^2	Determination coefficient
Ra	Arithmetic average of absolute roughness, µm
Rt	Maximum height of the roughness profile, µm
Rz	Average maximum height of the roughness profile, µm
T	Tool life, min
V	Cutting speed, m/min
$[VB]$	Admissible flank wear, 0.3 mm
Ve	Velocity of cutting vibration (RMS value), mm/s

Greek Symbols

α	Clearance angle, deg.
γ	Rake angle, deg.
λ	Cutting edge inclination angle, deg.
χ_r	Cutting edge angle, deg.

that is in competition to grinding [1-3]. It is also recommended as an economic and ecological process in the manufacturing industry. Although there are great advances in development of cutting tools such as ceramics, PCD and CBN there is still a great need in determining techniques for optimized use. So investigations are required on processes in order to improve tool lifetime, productivity and ensuring surface quality and geometrical tolerances. This will obviously lead to better understanding of the interaction between the machining parameters, the environment and the process tribology.

The interest to hard machining at high speeds grows fast therefore it becomes eminent to understand the behavior of the process through experimental and numerical modeling in order to optimizing the cutting regimes and conditions. For instance a material like AISI 52100 steel [4], with a good quenching ability and a hardness ranging from 60-68 HRC, has been a subject of large research investigation on hard machining that suggested the use of CBN and ceramics as performing tools [5, 6]. Moreover the effect of cutting parameters on the quality of a machined surface, cutting tool wear, productivity and choice of material and tool geometry is dominant in literature review [6-8]. The main results agree to conclude that cutting speed and hardness of the cutting tool are the most affecting parameters on the tool lifetime in hard turning of steel.

Attanasio et al. [9] have shown that flank wear rate is mainly affected by cutting speed and the crater wear rate is influenced by both cutting speed and feed rate. Meanwhile feed rate is reported to be most influencing on the surface roughness [10]. Kumar et al. [11] have shown that the flank wear of ceramic tool increases when cutting speed increases. Yellese et al. [12] have reported that when turning hardened AISI 52100 steel with CBN tools, cutting speeds beyond 280 m/min are neither productive nor qualitative but the radial force is most dominant cutting force and feed rate is most influencing parameter on surface roughness. In addition, from statistical and experimental analyses, Bouacha et al. [13] have indicated that the cutting force increases as feed rate and cutting depth increase

but it decreases when the cutting speed increases. Guddat et al. [14] have found that the insert type has significant effects on roughness rather than cutting speed.

Meddour et al. [15] have reported that the best surface roughness is obtained for small feed rate and large nose radius. Meanwhile, the influence of the depth of cut and cutting speed are very small when hard turning AISI 52100 steel. Moreover, when considering the cutting parameters, the machining time and tool wear [16], the analyses showed that roughness is slightly sensitive to the evolution of tool wear while wear is affected by the cutting speed and the machining time. In addition, with regard to temperature, Tanaka et al. [17] have shown that the cutting temperature increases of about 65 °C when tool wear increased from 0 to 0.1 mm in a range of cutting speeds of 100 to 150 m/min. In 2012, Hosseini et al. [18] have estimated a temperature of 1200 °C when the cutting speed reaches 260 m/min, but this has been corrected later in 2014 [19] to be about 900 °C. Bapat et al. [20] have shown that the cutting speed is the most influencing factor on the increase of cutting temperature: as the maximum temperature reaches 789 °C for a cutting speed 120 m/min, and 833 °C for a cutting speed of 200 m/min and 946 °C at 260 m/min.

Investigations on the bases of cutting vibrations have conducted to set some interesting correlation attempt. Dong et al. [21] have studied the correlation between surface roughness and cutting vibrations to develop an on-line roughness measuring technique in hard turning. On the basis of their theoretical analyses on the relationship between the cutting regimes, roughness and cutting tool vibrations, they have reported through their experimental investigation that the surface roughness along a workpiece has specific frequency range which could be used as a possible way to determine the correlation between cutting vibration and average surface roughness during hard turning. Kassab et al. [22] in their investigation on the effect of cutting tool vibration on surface roughness in dry turning of medium carbon steel have reported that the surface roughness of workpiece is proportional to cutting tool acceleration depending on the interaction of the cutting tool parameters. Meanwhile, they pointed out that feed rate has little effect on vibrations comparing to that of cutting speed and depth of cut. Moreover they suggested that vibration in axial direction could be neglect comparing to that of radial direction.

Upadhyay et al. [23] have attempted to use vibration signals for in-process prediction of surface roughness during turning of Ti-6Al-4V alloy. They have performed a correlation in order to determine the degree of association of 6 parameters; cutting speed, feed rate, and depth of cut and the acceleration amplitude of vibrations in axial, radial, and tangential directions with surface roughness. Using Pearson correlation coefficient for input parameters, they have neglected the acceleration amplitude of vibration in axial and the cutting speed. Therefore they refined their model according to feed rate that showed maximum correlation with surface roughness followed by acceleration amplitude of vibration in radial direction, depth of cut and acceleration amplitude of vibration in tangential direction. Sahoo et al. [24] have suggested an advanced hybrid multi output optimization technique by applying weighted principal component analysis (WPCA) incorporated with response surface methodology (RSM) in order to optimize surface roughness and tool vibration in CNC turning of Aluminum alloy 63400. Through ANOVA analysis, they have revealed that feed rate and second order term of spindle speed are most influencing parameter for surface roughness and tool vibration respectively.

Manivel et al. [25] have developed prediction models for radial and tangential acceleration amplitude tool vibration in hard turning of austempered ductile iron grade 3. They have reported that in the tangential direction, the cutting speed is most affecting tool vibration with the 54% contribution while feed rate and depth of cut contributed respectively with 27% and 19%. In the radial direction, the influence of cutting speed is weak with only 12% comparing to depth of cut and feed rate with respective contributions of 74% and 14%. They have also proposed a regression prediction model for tool vibration behavior. Hessainia et al. [26] in their research work on the prediction of surface roughness in the hard turning as a function of cutting parameters and tool vibrations in the axial and radial directions have developed a surface roughness model using the response surface methodology (RSM). They reported that feed rate is the most dominant factor affecting surface roughness comparing to cutting vibrations concluding that the effect of vibration is minor. Izelu et al. [27] have presented a machining induced vibration and surface roughness models to predict and optimize the cutting tool overhang, feed rate and cutting speed during hard turning of 41Cr4 alloy structural steel at high speed. Using surface response methodology, they have developed an empirical model relating machining induced vibration and surface roughness that they suggested to be accurate and reliable. However, the relationship is nonlinear and shows no significant correlation within the experimental design limits. Plaza et al. [28] have assessed two methods for enhanced surface roughness monitoring based on the application of singular spectrum analysis to vibrations signals generated in workpiece-cutting tool interaction in CNC finish turning operations. They have concluded that singular spectrum analysis is an ideal method for analyzing vibration signals applied to the on-line monitoring of surface roughness. There is still a great deal in literature [29-34] on the behavior of hard machining as research work is oriented to morphology of chip, residual stresses, cooling, environment surface integrity, tool wear, surface quality, tool geometry and particularly technological parameters. In the above reviewed literature most of the investigations on the correlation between cutting vibrations and surface roughness have been conducted on ductile materials and on materials with lower hardness at cutting speed below 180 m/min. Moreover, the significant correlation has been obtained using Pearson correlation coefficient [23].

The present work is a contribution in determining a correlation between surface roughness and cutting vibrations during hard turning of AISI 52100 steel (66 HRC) at higher cutting speed (up to 280 m/min). First, investigation on wear in mixed ceramic tool when machining has been conducted. Then, Taguchi's L_{27} (3^3) orthogonal array has been proposed to analyze roughness and cutting vibrations as a function of cutting parameters. Finally, the main objective of the present work is to determine a realistic correlation model between surface roughness and cutting vibration using Pearson correlation method supported by Spearman coefficient method.

2. Experimental Procedure

2.1. Specimen preparation

A grade AISI 52100 steel (100Cr6 according to DIN) characterized by an important quenching ability and good resistance to wear has been used. It is commonly used for manufacturing bearing balls, rollers, rings, bearing cages and

also as tool material in cold forming such as dies, rolling mills calibers. The chemical composition identified by an optical emission spectrometer (Thermo Scientific ARL 4460) is illustrated in Table 1.

Table 1. Chemical composition of grade AISI 52100 steel in weight %.

Element	C	Mn	Si	Ni	Al	Cr	V	Ti	Mo
Composition	0.939	0.277	0.265	0.175	0.012	1.444	0.004	0.005	0.058

Hardening of the material has been achieved on a round bar blank of 130 mm diameter and 360 mm length by quenching from 850 °C in oil bath and then tempering at 200 °C for 2 hours. The heat treatment has been conducted using an electric oven type WOT 9703- 457 404 with maximum heating temperature of 1600 °C. Hardness values after tempering, measured with a Hardness Testing HLM-100 Plus device have reached 66 ± 1HRC.

2.2. Cutting inserts

Eight square working edges removable cutting inserts of the designation SNGN 120408 have been used. They are made of mixed ceramics (CC650) made of (70% Al_2O_3 + 30% TiC). They are mounted on a tool holder PSBNR2525M12 of the following geometry: χ_r = 75°; α = 6°; γ = -6°; λ = -6°.

2.3. Measuring Instruments

A CCD camera equipped optical microscope type HUND (W-AD) has been used to measure wear in cutting tools. Computer image analyses have been completed using Motic 2000 software.A Vibration Digital Meter (VM-6360), with measuring ranges: 0-199 mm/s velocity, 0-20 g acceleration and 1-1999 µm displacement has been set to record vibration signals in cutting tool. Radial vibrations have been recorded by mounting a uni-axial accelerometer sensor the tool holder in the radial direction. Meanwhile, a Surftest 301 Mitutoyo roughness meter has been employed to measure roughness on the machined surface.

2.4. Cutting conditions

Machining has been performed in dry conditions on a SN40 parallel Lathe with a spindle power of 6.6 kW and a maximum rotational speed of 2000 rev/min. The blank has been mounted in between chuck and centre. Two distinctive series of experimentation tests characterized the present work. The first series consisted in determining the lifetime of the cutting tool. The latter has been conducted using uni-factorial experiment plan where the cutting speed and feed rate have been varied while the depth of cut is maintained constant with a small value as suggested in literature [35]. The depth of cut in the present work corresponded to a constant value of 0.3 mm through the first series of experimentation. Table 2 summarizes the cutting conditions for tool lifetime investigation. The lifetime is assigned to the evolution of flank wear of the tool cutting edge. This evolution is obtained by first increasing the cutting speed and fixing the feed rate constant. The cutting speed started from 140 m/min corresponding to a convenient cutting speed for long tool life as reported in literature and ended when wear is very fast, while the feed rate has been set to its minimum value of 0.08 mm/rev. Then, the flank wear evolution is determined as a function of feed rate by adapting a constant cutting speed. A cutting speed of 200 m/min has been adapted.

The second series of experimentation has been carried out using a L_{27} full factorial design (27 combinations) and analysis of variance (ANOVA) with 26 degrees of freedom in order to investigate the effect of cutting parameters (cutting speed, feed rate, and depth of cut) on the surface roughness and the tool radial vibrations during machining and then to establish a corresponding correlation. Table 3 shows levels of combination of the cutting parameters.

Table 2. Uni-factorial plan for mixed ceramics (CC650) wear investigation.

Cutting Parameters	**Unit**	**Levels of parameters variation (factors)**							
Cutting Speed (*V*)	m/min	140	200	280	380	530	200	200	200
Feed (*f*)	mm/rev	0.08	0.08	0.08	0.08	0.08	0.12	0.16	0.22
Depth of cut (*a*)	mm	0.3	0.3	0.3	0.3	0.3	0.3	0.3	0.3

Table 3. Levels of the cutting parameters' variation for the factorial plan L_{27}.

Cutting Parameters	***Unit***	***Levels***		
		-1	**0**	**1**
Cutting Speed (*V*)	m/min	140	210	280
Feed (*f*)	mm/rev	0.08	0.16	0.22
Depth of cut (*a*)	mm	0.15	0.325	0.5

3. Results and Discussion

3.1. Tool life model

Figure 1 shows plots of measured wear on the flank of the cutting edge of the tool as a function of time. The effect of the cutting speed is illustrated by increasing its value from 140 to 530 m/min (keeping the feed rate and depth of cut at a constant value of 0.08 mm/rev and 0.3 mm, respectively). In each cutting speed condition, wear test is stopped when the critical wear value *[VB]* = 0.3 mm is reached. So the tool lifetime corresponds to the time by the critical wear is obtained. Basically, the usual wear trend is observed for the 5 investigated cutting speeds, however as the cutting speed increases, wear increases drastically as presented in Table 4. Increasing the speed from 140 m/min to 530 m/min, lifetime falls down of 8.75 times. Figure 2 shows the rate of reduction in tool lifetime as a function of cutting speed. Above 280 m/min tool lifetime decreases drastically when the curve trend slopes down. This can be explained by the fact that when the temperature in the cutting zone rises rapidly and considerably affecting the heat resistance of the tool material generating different wear mechanisms of the cutting tool (abrasion, adhesive, diffusion...) that heavily reduce the lifetime of the tool. In addition to the effect of cutting speed on temperature, there appears another phenomenon of instability of the machining system, which is induced by the increase in the vibration amplitude as the rotational frequency increase as shown in Fig. 3. The combination of these two phenomena contributes to the acceleration of the tool wear.

Table 4. Effect of cutting speed on of mixed ceramics (CC650) lifetime.

Speed *V*(m/min)	**Lifetime of tool *T*(min)**	**Rate of lifetime (T_{vx}/T_{140})**	**Degradation Rate of *T* (T_{140}/T_{vx})**
140	35	(100%)	(1)
200	28	80%	1.25
280	16	45%	2.19
380	11	31%	3.18
530	4	10%	8.75

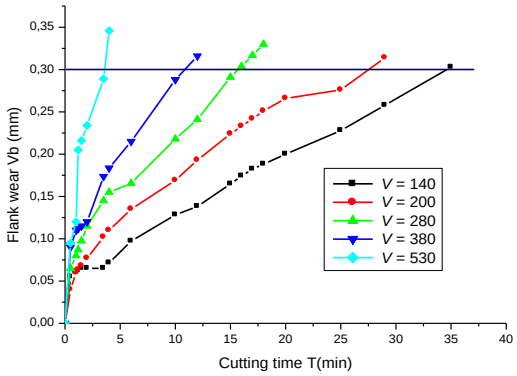

Fig. 1. Effect of cutting speed on flank wear in mixed ceramics (CC650) when turning of hardened steel AISI 52100 (*f* = 0.08 mm/rev and *a* = 0.3 mm).

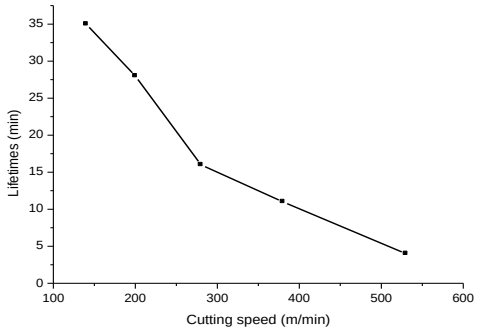

Fig. 2. Evolution of mixed ceramics (CC650) lifetime as a function of cutting speed (*f* = 0.08 mm/rev and *a* = 0.3 mm).

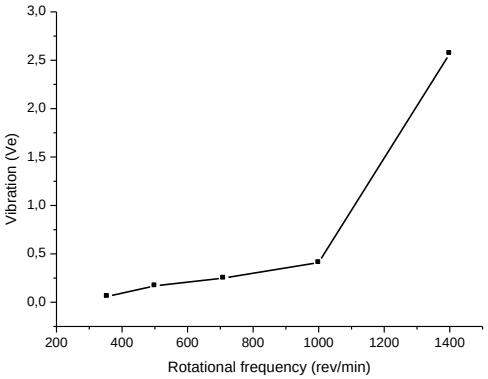

Fig. 3. Vibration in unloaded machine tool as a function of spindle frequency.

Multiple second order regression equation has been implemented at 95% confidence level to obtain the correlation between the tool life (T) in min and the cutting speed (V) in m/min and expressed by Eq. (1):

$$T = 0.000172V^2 - 0.194V + 58.54 \quad (1)$$

With: $R^2 = 98.98\%$; (f = 0.08 mm/rev and a = 0.3 mm).

Predicted values and measured values for both responses are very close to each other as shown in Table 5. So, the engineering model in Eq. (1) can be used as an accurate tool life prediction in hard turning using mixed ceramic insert when turning with low values of feed and depth of cut.

Table 5. Comparison between measured and predicted tool life values as a function of cutting speed.

Cutting speed *V*(m/min)	Experimental Value *T*(min)	Predicted 2nd order model Value	Residuals
140	35	34.71	0.29
200	28	26.56	1.44
280	16	17.62	-1.62
380	11	9.54	1.46
530	4	3.87	0.13

The effect of feed rate on tool lifetime is shown in Figs. 4 and 5. Increasing Feed rate of 2.75 times from 0.08 to 0.22 mm/rev resulted in a decrease of lifetime by 29%, from 28 to 20min, (Table 6). The degree of feed influence is relatively lower comparing to cutting speed. The present results are in good agreement with those reported in literature [9, 36, 37]. It should also be noted that changes in the lifetime of the tool decrease according to the increase in the feed rate specifically at 0.16 mm/rev. Then, this effect becomes relatively less pronounced (Fig. 5). Applying multiple second order regression equation on the tool lifetime (T), min as a function of feed rate (f), mm/rev, then Eq. (2) is obtained:

$$T = 215.16 f^2 - 117.82 f + 35.80 \quad (2)$$

With: R^2 = 99.57%; (V= 200 m/min and a = 0.3 mm).

Again, the predicted values and measured values for both responses are very close to each other (Table 7) with maximum residuals of only 0.46.

Table 6. Effect of feed rate on of mixed ceramics (CC650) lifetime.

Feed rate *f*(mm/rev)	Lifetime of tool *T*(min)	Rate of lifetime (T_{fx} /$T_{0.08}$)	Degradation Rate of T ($T_{0.08}$/T_{fx})
0.08	28	(100%)	(1)
0.12	25	90%	1.12
0.16	22	79%	1.27
0.22	20	71%	1.40

Table 7. Comparison between measured and predicted tool life value as a function of feed rate.

Feed rate *f*(mm/rev)	Experimental Value *T*(min)	Predicted 2nd order model Value	Residuals
0.08	28	27.75	0.25
0.12	25	24.76	0.24
0.16	22	22.46	-0.46
0.22	20	20.29	-0.29

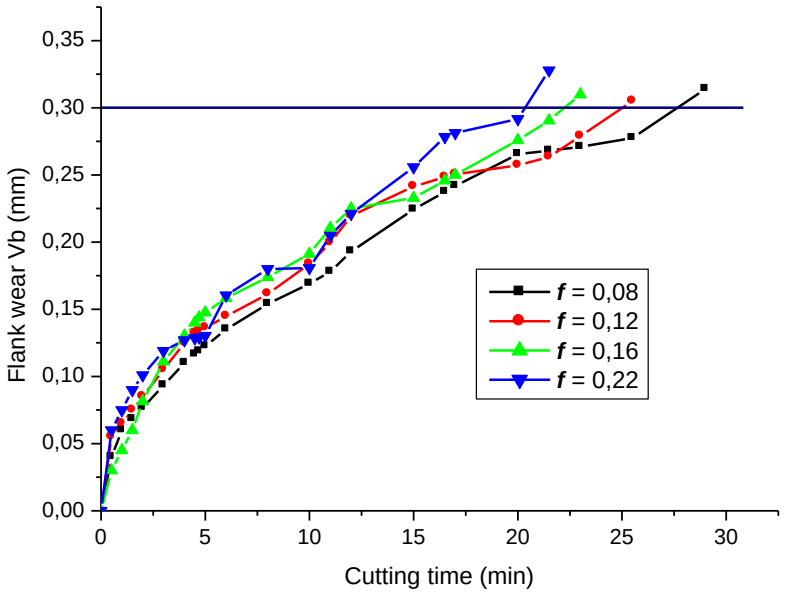

Fig. 4. Effect of feed rate on flank wear in mixed ceramics (CC650) when finish turning of hardened steel AISI 52100 (*V* = 200 m/min and *a*= 0.3 mm).

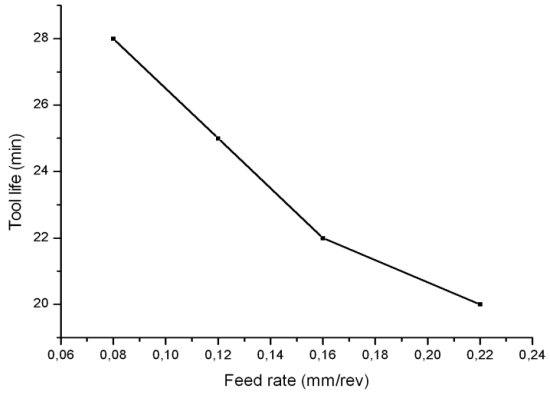

Fig. 5. Evolution of mixed ceramics (CC650) lifetime as a function of feed rate

The morphology of tool wear is shown in Fig. 6. When the cutting speed increases from 200 to 530 m/min, Fig. 6(a), wear grows and shows a type of collapse of the tool nose, characterized by abrasion streaks and a significant loss of material on the flank face, and on the attack surface (Fig. 7). With regards to the effect of feed rate on the morphology, Fig. 6(b), the degradation in the tool nose occurs in the form of a cavity characterized by streaks and burns. In both cases, no chipping or breakage was visible on the cutting edges (Figs. 6 and 7), indicating that the stiffness of the workpiece and tool fixture system was suitable for the machining. This is also supported by a high chemical stability of ceramics. The scratches parallel to the cutting direction caused by the friction phenomenon reveals that wear is mainly abrasive. This is in good agreement with results given in literature [38, 39].

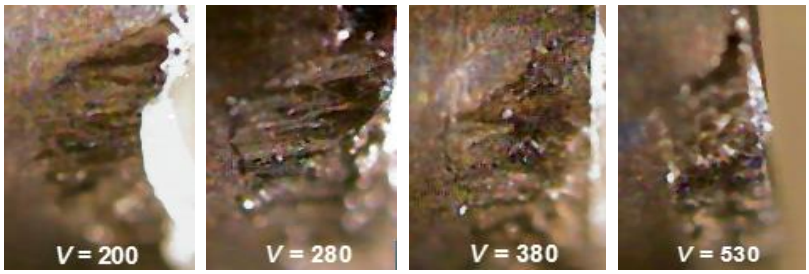

(a)With: f = 0.08 mm/rev and a = 0.3 mm.

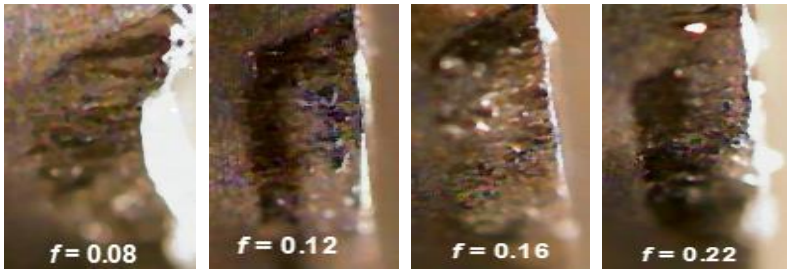

(b)With: V = 200 m/min and a = 0.3 mm.

Fig. 6. Morphology of flank wear of the cutting tool CC650 according to the cutting speed (a) and as a function of feed rate (b).

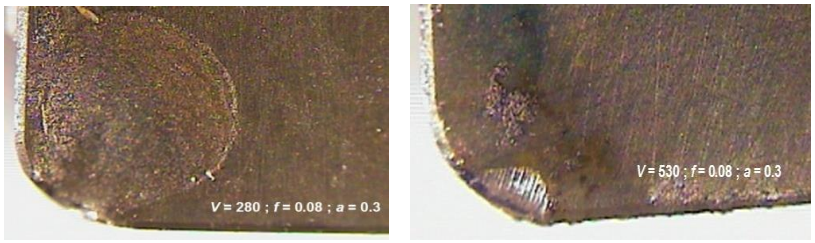

Fig. 7. Morphology of crater wear in the cutting tool CC650 (for two cutting speed: 280 m/min and 530 m/min).

3.2. Surface roughness and radial vibrations

Experimental values of roughness and radial cutting vibrations during hard turning of AISI 52100 steel by CC650 tool were obtained by varying the cutting conditions based on exploratory experiments and literature review. A series of tests was conducted according to orthogonal array L_{27} of Taguchi experiment design with three variables and three levels. The objectives of the statistical analysis is to determine in one hand the effect of cutting parameters on the technological parameters, for instance the roughness of the machined surface and radial vibrations of the tool nose and in the other hand the correlation between them. Table 8 gives the respective experimental results of surface roughness (*Ra*, *Rz* and *Rt*) and radial cutting vibrations.

Table 8. Surface roughness and cutting radial vibrations according to orthogonal array L_{27} of Taguchi experiment design.

	Cutting Parameters			Roughness			Vibration
Test N°	***a*** **(mm)**	***V*** **(m/min)**	***f*** **(mm/rev)**	***Ra*** **(µm)**	***Rz*** **(µm)**	***Rt*** **(µm)**	***Ve*** **(mm/s)**
1	0.15	140	0.08	0.87	5.51	6.74	0.199
2	0.15	140	0.16	1.37	6.74	7.61	0.207
3	0.15	140	0.22	1.98	9.69	10.51	0.241
4	0.15	210	0.08	1.24	6.03	6.98	0.368
5	0.15	210	0.16	1.29	6.79	8.22	0.413
6	0.15	210	0.22	1.82	9.36	10.53	0.495
7	0.15	280	0.08	1.03	4.88	5.29	0.495
8	0.15	280	0.16	1.18	5.77	6.53	0.520
9	0.15	280	0.22	1.87	9.28	9.75	0.550
10	0.33	140	0.08	0.93	5.21	6.28	0.204
11	0.33	140	0.16	1.58	7.99	8.71	0.239
12	0.33	140	0.22	2.04	9.57	10.80	0.245
13	0.33	210	0.08	1.43	7.14	8.27	0.468
14	0.33	210	0.16	1.75	9.14	10.46	0.479
15	0.33	210	0.22	2.21	10.54	12.35	0.536
16	0.33	280	0.08	1.24	6.86	8.02	0.549
17	0.33	280	0.16	1.43	7.53	8.85	0.554
18	0.33	280	0.22	2.15	10.70	11.86	0.573
19	0.5	140	0.08	1.15	5.90	7.40	0.332
20	0.5	140	0.16	1.66	8.12	8.78	0.550
21	0.5	140	0.22	2.47	10.96	11.65	0.686
22	0.5	210	0.08	1.09	5.94	6.77	0.483
23	0.5	210	0.16	1.57	7.65	5.24	0.580
24	0.5	210	0.22	2.44	10.34	10.88	0.704
25	0.5	280	0.08	0.98	5.23	6.57	0.466
26	0.5	280	0.16	1.45	7.52	8.52	0.526
27	0.5	280	0.22	2.27	9.64	10.25	0.573

3.2.1. ANOVA for the surface roughness (*Ra*)

The best value of the surface roughness (*Ra*) is obtained with the combination of: cutting speed, 140 m/min feed rate, 0.08 mm/rev and depth of cut, 0.15 mm. This is explained by the slow elimination of small chip thickness, resulting in a continuous removal of the material that contributes to the improvement of surface quality. However, the highest value of roughness is observed for high feed rate of 0.22 mm/rev. This is explained by the rapid removal of matter, the change of the chip morphology (Fig. 8) and the distance between the scratches that degrade the machined surface. At lower feed rate, continuous chips have been obtained because the material is sufficiently deformable and the friction between cutting tool and chip was uniform generating deformed structure of the chip material [33]. So, they are most desirable chip type contributing in improving the surface quality. At higher feed rate as the cutting force and compressive stresses increased, the chips were segmented resulting in discontinuous chip type that has been torn off from the surface [40].

Analysis of variance (ANOVA) has been also been used on test results given in Table 8, in order to identify the most significant factors affecting surface roughness, using significance level of α=0.05, i.e. for a confidence level of 95%.

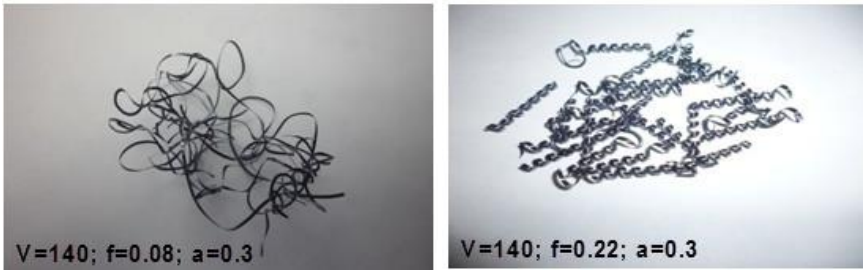

Fig. 8. Effect of feed on the chip shape.

Table 9(a) illustrates ANOVA results for surface roughness revealing that feed parameter (*f*) is the most statistically significant parameter at a contribution rate of 83.84% then follows the cutting depth with (6.65%), whereas the interaction (*a*f*) contributes only 3.49% and cutting speed 1.51%. Interactions (*a*V*) and (*f *V*), considered statistically not significant, with contribution rates 1.81% and 1.71%, respectively. We can say that their effect on the roughness is negligible. The error contribution for surface roughness (*Ra*) is very small with contribution of 1% which means that the three cutting parameters (cutting speed, feed rate and depth of cut) are sufficient enough to predict the roughness (*Ra*).

The analyses of the main effects on the roughness of the machined surface have been conducted with the software package MINITAB16. Results are illustrated in Fig. 9. Depth of cut and cutting speed show a slight influence on the surface roughness. When increasing the depth of cut, there is a slight increase of roughness and when increasing cutting speed, roughness increases first up to a cutting speed of 210 m/min, then decreases for higher speeds (210 to 280 m/min). However, the effect of the feed is remarkable and relatively more pronounced (Fig. 9). The minimum values of roughness are obtained for low feed and small depths. These results are in good agreement with literature [41-45].

3.2.2. ANOVA for radial vibrations (*Ve*)

Experimental RMS values of velocity amplitude shown in Table 8. At low depth of cut, radial force becomes dominant when compared to the other components of cutting force [12, 13, 34] which is reflected by the important values of vibration in the radial direction [37]. Low velocity value is recorded for low cutting conditions (V = 140 m/min; f = 0.08 mm/rev; a = 0.15 mm) because low radial force is required for slow removal of small chip thickness. High velocities are obtained for high cutting speeds, feeds and higher depths. In this case, significant radial force is generated during the rapid removal of an important volume of matter. In addition, this is combined with parasites of vibrations generated by the spindle frequency (Fig. 3).

Statistical analysis of radial vibration results presented in Table 9(b) shows that the cutting speed (*V*) is the most significant parameter with a contribution rate of 41.32% followed by the depth of cut (21.11%) and feed (10.59%). This is due to the contribution of the total vibrations of the machining system for high rotation frequencies (Fig. 3). The contribution of the error is low (2.11%). The analysis of the main effects on radial vibration is shown in Fig. 10. Vibrations increase when cutting parameters (speed, feed and depth) increase. Minimum vibration values are obtained at low cutting parameter levels because the cross-

section of the chip is minimal which can be easily removed at low cutting force. As a result, the machining system becomes stable.

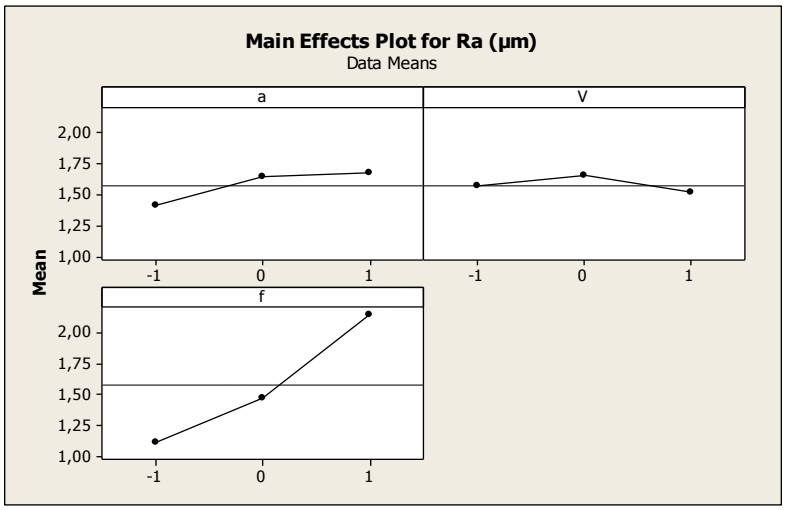

Fig. 9. Main effect on the surface roughness (*Ra*).

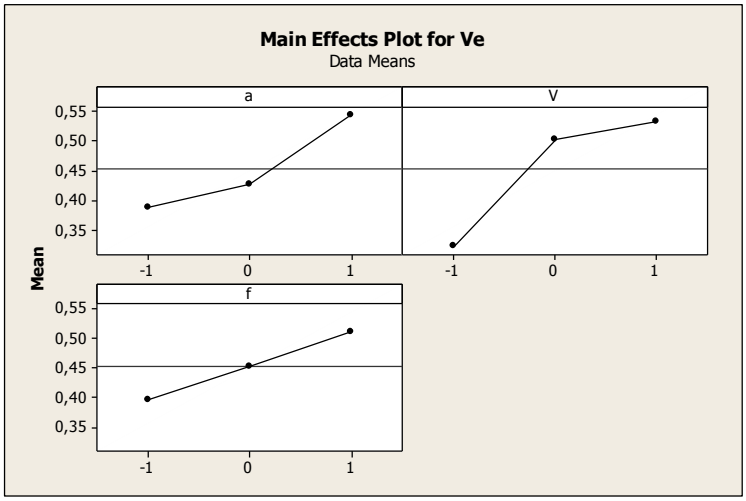

Fig. 10. Main effect on the radial vibration (*Ve*).

Table 9(a). Analysis of variance of the surface roughness (*Ra*).

Source	SS	DOF	MS	F - Value	P	%C
a	0.39188	2	0.19594	26.56	0.000	6.65
f	4.94382	2	2.47191	335.10	0.000	83.84
V	0.08903	2	0.04452	6.03	0.025	1.51
a * V	0.10666	4	0.02667	3.61	0.058	1.81
f * V	0.10103	4	0.02526	3.42	0.065	1.71
a * f	0.20551	4	0.05138	6.96	0.010	3.49
Error	0.05901	8	0.00738			1
Total	5.89696	26				

S = 0.0858879 **R-Sq** = 99.00% **R-Sq(adj)** = 96.75%

Table 9(b). Analysis of variance of cutting vibration (*Ve*).

Source	SS	DOF	MS	F - Value	P	%C
a	0.119796	2	0.059898	40.02	0.000	21.11
f	0.060107	2	0.030054	20.08	0.001	10.59
V	0.234493	2	0.117246	78.34	0.000	41.32
a x V	0.103969	4	0.025992	17.37	0.001	18.32
f x V	0.007574	4	0.001893	1.27	0.359	1.33
a x f	0.029541	4	0.007385	4.93	0.027	5.21
Error	0.011973	8	0.001497			2.11
Total	0.567453	26				

S = 0.0386857 **R-Sq** = 97.89% **R-Sq(adj)** = 93.14%

3.2.3. 3D surface plots of surface Roughness and radial vibrations

The impact and the degree of influence of cutting parameters (*V*, *f* and *a*) on the surface roughness and the radial vibration are presented in Fig. 11 which illustrates 3D surface plot responses versus different combinations of cutting parameters. For each plot, the non presented variables are held at a constant mean value. With regards to surface roughness, feed rate is the most influencing parameter. With regards to vibrations, cutting speed has great effect. So, (Fig. 11) confirm the nodes observed during the principal effects plots analysis.

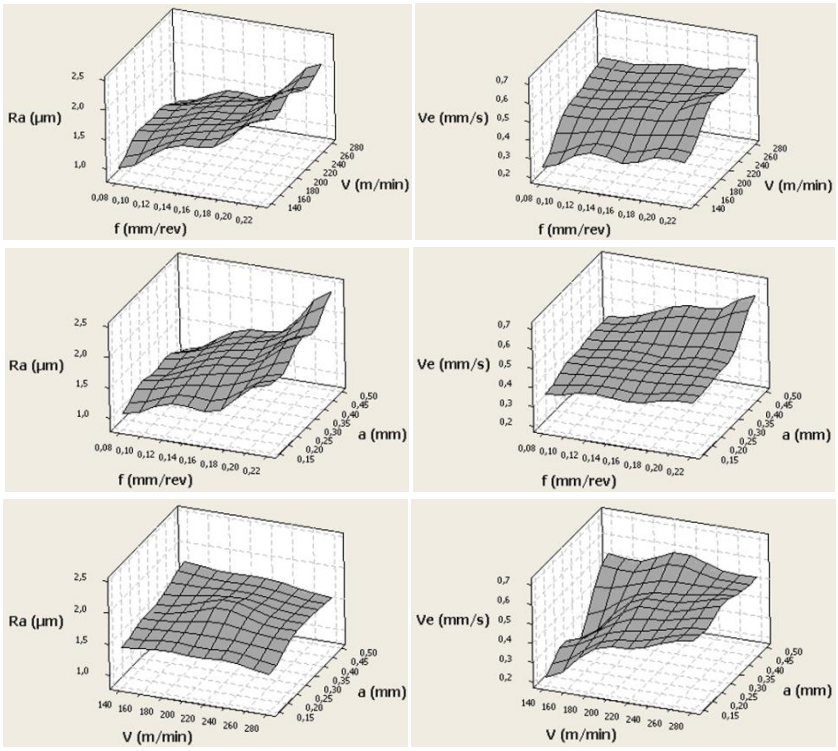

Fig. 11. 3D surface plots of Roughness and radial vibrations.

3.2.4. Models for surface roughness and radial vibration

Multiple second order regression models has been implemented at 95% confidence level to obtain the correlation between cutting parameters and technological parameters, surface roughness (*Ra*) and Radial vibration (*Ve*). The corresponding engineering expressions are given in Eqs. (3) and (4):

$$Ra = 1.62 - 0.1a^2 - 0.114V^2 + 0.147f^2 + 0.119af - 0.036aV - 0.042Vf - 0.136a - 0.025V + 0.517f \quad (3)$$

with: $R^2 = 95.5\%$.

$$Ve = 0.475 + 0.039a^2 - 0.074V^2 + 0.002f^2 + 0.039af - 0.076aV - 0.02Vf + 0.078a + 0.105V + 0.057f \quad (4)$$

with: $R^2 = 89.3\%$.

The regression analysis of the surface roughness model is shown in Table 10(a). The multiple correlation coefficient (R^2) is very acceptable, confirming the suitability of the multiple regression equation. The ANOVA of regression for *Ra* shows a P-value (probability signification) lower than 0.05. This means that the terms mentioned in the model have significant effects on the response of *Ra*. For the regression model of vibrations, the analysis is presented in Table 10(b). The R^2 value is acceptable, and the P-value shows that the model is significant.

Table 10(a). ANOVA regression analysis of surface roughness (*Ra*).

Source	SS	DOF	MS	F - Value	P	Remark
Regression	5.63087	9	0.62565	39.97	0.000	Significant
Residual Error	0.26608	17	0.01565			
Total	5.89696	26				
S = 0.125108	**R-Sq** = 95.5%		**R-Sq(adj)** = 93.1%			

Table 10(b). ANOVA regression analysis of cutting vibration (*Ve*).

Source	SS	DOF	MS	F - Value	P	Remark
Regression	0.503630	9	0.055959	15.72	0.000	Significant
Residual Error	0.060533	17	0.003561			
Total	0.564163	26				
S = 0.0596723	**R-Sq** = 89.3%		**R-Sq(adj)** = 83.6%			

The validation of data obtained from models (3) and (4), are given by the average percentage error for second order models of roughness (*Ra*) and velocity radial vibrations which were respectively 6.2% and 10.3%, Tables 11(a) and (b). The percentage error was calculated by the following relation in Eq. (5):

$$\%error = \frac{Experimental - \mathrm{Predicted}}{Experimental} \times 100 \quad (5)$$

3.3. Correlation between surface roughness and radial vibrations

In order to find the qualitative and quantitative correlation between the surface roughness and the radial vibration, a comparative analysis of the trends of roughness

change (*Ra*) and those of the radial vibration (*Ve*) has been made (Fig. 12). When increasing cutting speed, roughness decreases, while the vibrations increase. This is explained by the fact that at high rotational frequencies of the spindle, the vibrations increase (Fig. 3). The analysis also shows that when feed and depth of cut increase, roughness and vibration tend to increase but with relatively low rates.

Pearson's coefficient expressing the correlation between roughness (*Ra*) and vibration (*Ve*) is equal to 0.465 and that of Spearman is equal to 0.554, which shows that the linear or non-linear correlation between these two parameters is low. This hypothesis is confirmed by the correlation diagram shown in Fig. 13, where the cloud of the points illustrates a remarkable dispersion.

Table 11(a). Predicted values and their percentage error for *Ra*.

Test N°	**Experimental Value *Ra***	**Predicted 2nd order model Value**	**% Error in value predicted**	*Test N°*	***Experimental Value Ra***	***Predicted 2nd order model Value***	***% Error in value predicted***
1	0.87	0.9668	-11.13	15	2.21	2.2804	-3.19
2	1.37	1.2581	8.17	16	1.24	1.1520	7.10
3	1.98	1.8440	6.87	17	1.43	1.4793	-3.45
4	1.24	1.1329	8.64	18	2.15	2.1009	2.28
5	1.29	1.3826	-7.18	19	1.15	1.0718	6.80
6	1.82	1.9268	-5.87	20	1.66	1.6015	3.52
7	1.03	1.0734	-4.21	21	2.47	2.4256	1.80
8	1.18	1.2815	-8.60	22	1.09	1.1645	-6.83
9	1.87	1.7840	4.60	23	1.57	1.6526	-5.26
10	0.93	1.1187	-20.29	24	2.44	2.4351	0.20
11	1.58	1.5293	3.21	25	0.98	1.0318	-5.29
12	2.04	2.2353	-9.57	26	1.45	1.4781	-1.94
13	1.43	1.2481	12.72	27	2.27	2.2190	2.25
14	1.75	1.6170	7.60				

Average percentage error = 6.24%

Table 11(b). Predicted values and their percentage error for *Ve*.

Test N°	**Experimental Value *Ve***	**Predicted 2nd order model Value**	**% Error in value predicted**	*Test N°*	***Experimental Value Ve***	***Predicted 2nd order model Value***	***% Error in value predicted***
1	0.199	0.1403	29.50	15	0.536	0.5355	0.09
2	0.207	0.1791	13.48	16	0.549	0.4721	14.01
3	0.241	0.2213	8.17	17	0.554	0.5071	8.47
4	0.368	0.4183	-13.67	18	0.573	0.5457	4.76
5	0.413	0.4361	-5.59	19	0.332	0.3744	-12.77
6	0.495	0.4274	13.66	20	0.550	0.4895	11.00
7	0.495	0.5471	-10.53	21	0.686	0.608	11.37
8	0.520	0.544	-4.62	22	0.483	0.4989	-3.29
9	0.550	0.5444	1.02	23	0.580	0.593	-2.24
10	0.204	0.2188	-7.25	24	0.704	0.6906	1.90
11	0.239	0.2957	-23.72	25	0.466	0.4741	-1.74
12	0.245	0.3761	-53.51	26	0.526	0.5474	-4.07
13	0.468	0.42	10.26	27	0.573	0.6241	-8.92
14	0.479	0.476	0.63				

Average percentage error = 10.37%

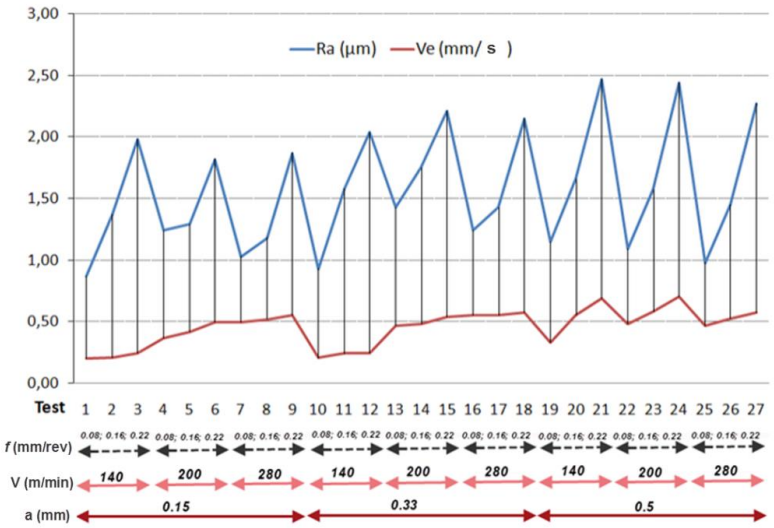

Fig. 12. Trend changes in surface roughness (*Ra*) and Radial vibrations (*Ve*) for the 27 combinations of the experimental design.

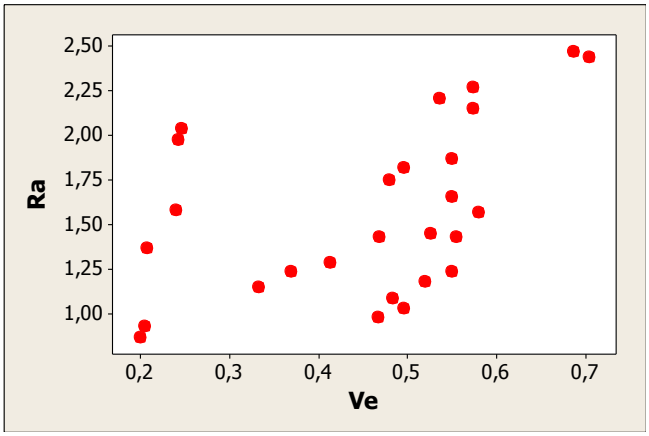

Fig. 13. Intensity of the relationship between the roughness (*Ra*) and the radial vibrations (*Ve*).

4. Conclusions

The present work is a contribution to determining the correlation of roughness and tool radial vibration when hard turning of hardened AISI 52100 steel (66 ±1HRC) using the mixed ceramic (70% Al_2O_3 + 30% TiC). Wear has been first investigated in order to sort out an experimental plan to carry out the present investigation. The main conclusions are:

- The combination of cutting conditions (V = 140 m/min; f = 0.08 mm/rev; a = 0.3 mm) resulted in best tool life with 35 minutes for an admissible wear 0.3 mm.
- Increasing cutting speed (3.78 times) reduced the tool lifetime by 8.75 times.

- Increase feed by 2.75 times led to the 29% reduction of tool lifetime.
- Abrasion wear has been dominant on the active surfaces of the tool.
- Feed is the dominant factor affecting on the machined surface roughness (*Ra*) with a contribution rate of 83.84%.
- The best surface quality has been observed for the combination of experimental design (V = 140 m/min, f = 0.08 mm/rev and a = 0.15 mm).
- Multiple second order regression model for the surface roughness has been adopted with high coefficient of determination R^2 (R^2 = 0.955), which is a reliable response to 95.5%.
- Up to 1000 rev/min, a "free driving" test revealed that when the rotation frequency (N) of the spindle increases by 3 times vibrations are 4 times higher. In the range of higher frequencies (1000 to 1400 rev/min), 1.4 times increase in N, induces an increase of radial vibration of 6.5 times.
- High speeds for hard turning generate additional parasitic vibrations. So the most significant effect on the radial vibration is attributed to the cutting speed.
- The coefficients of linear or nonlinear correlation between roughness and radial vibrations are low because of the instability of the machining system at high rotational frequencies. However Spearman coefficient is higher than Pearson coefficient with respective values of 0.554 and 0.465.

Acknowledgments

The present work has been conducted within CNEPRU Research Project-LRTAPM: A11N01UN230120130011 (Badji Mokhtar - Annaba University). The authors would like to thank the tutorship of the research project, the Algerian Ministry of Higher Education and Scientific Research (MESRS) and the Delegated Ministry for Scientific Research (MDRS) for financial support.

References

1. Schultz, H. (1997). State of the art of high speed machining. *First French and German Conference of High Speed Machining*. Metz, France, 1-7.
2. Schneider Jr, G. (2002). Cutting tool applications. *Prentice-Hall Publication*, Chapter 1, 2-65.
3. Poulachon, G.; and Moison, A. (2003). Performance evaluation on hardened steel-PCBN tool pair in high speed turning. *Matériaux & Techniques*, 91(1), 23-44.
4. Poulachon, G.; Moisan, A.; and Jawahir, I.S. (2001). On modelling the influence of thermo-mechanical behaviour in chip formation during hard turning of 100Cr6 bearing steel. *CIRP Annals-Manufacturing Technology*, 50(1), 31-36.
5. Huang, Y.; and Dawson, T.G. (2005). Tool crater wear depth modelling in CBN hard turning. *Wear*, 258(9), 1455-1461.
6. Benga, G.C.; and Abrao, A.M. (2003). Turning of hardened 100Cr6 bearing steel with ceramic and PCBN cutting tools. *Journal of Materials Processing Technology*, 143, 237-241.

7. Chou,Y.K.; Evans, C.J.; and Barash, M.M. (2002). Experimental investigation on CBN turning of hardened AISI 52100 steel. *Journal of Materials Processing Technology*, 124(3), 274-283.
8. Ozel, T.; Hsu, T.K.; and Zeren, E. (2005). Effects of cutting edge geometry, workpiece hardness, feed rate and cutting speed on surface roughness and forces in finish turning of hardened AISI H13 steel. *International Journal of Advanced Manufacturing Technology*, 25(3), 262-269.
9. Attanasio, A.; Umbrello, D.; Cappellini, C.; Rotella, G.; and M'Saoubi, R. (2012). Tool wear effects on white and dark layer formation in hard turning of AISI 52100 steel. *Wear*, 286, 98-107.
10. Riza, A.M. (2011). Tool life performance, wear mechanisms and surface roughness characteristics when turning austenised and quenched AISI 52100 bearing steel with ceramic and CBN/TiC cutting tools. *Indian Journal of Engineering & Materials Sciences*, 18, 137-146.
11. Kumar, A.S.; Durai, A.R.; and Sorna, K.T. (2006). Wear behavior of alumina based ceramic cutting tools on machining stainless steel and EN24 steel. *Tribology International*, 39 (2), 191-197.
12. Yallese, M.A.; Chaoui, K.; Zeghib, N.; and Boulanouar, L. (2009). Hard machining of hardened bearing steel using cubic boron nitride tool. *Journal of Materials Processing Technology*, 209(2), 1092-1104.
13. Bouacha, K.; Yallese, M.A.; Mabrouki, T.; and Rigal, J.F. (2010). Statistical analysis of surface roughness and cutting forces using response surface methodology in hard turning of AISI 52100 bearing steel with CBN tool. *Journal of Refractory Metals & Hard Materials*, 28(3), 349-361.
14. Guddat, J.; M'Saoubi, R.; Alm, P.; and Meyer, D. (2011). Hard turning of AISI 52100 using PCBN wiper geometry inserts and the resulting surface integrity. *Procedia Engineering*, 19, 118-124.
15. Meddour, I.; Yallese, M.A.; Khattabi, R.; Elbah, M.; and Boulanouar, L. (2015). Investigation and modeling of cutting forces and surface roughness when hard turning of AISI 52100 steel with mixed ceramic tool: cutting conditions optimization. *International Journal of Advanced Manufacturing Technoloy*, 77(5), 1387-1399.
16. Bouacha, K.; Yallese, M.A.; Khamel, S.; and Belhadi, S. (2014). Analysis and optimization of hard turning operation using cubic boron nitride tool. *International Journal of refractory Metals and Hard Materials*, 45, 160-178.
17. Tanaka, R.; Motishita, H.; Lin, Y.; Hosokawa, A.; Ueda, T.; and Furumoto, T. (2009). Cutting tool edge temperature in finish hard turning of case hardened steel. *Key Engineering Materials*, 407(408), 268-272.
18. Hosseini, S.B.; Ryttberg, K.; Kaminski, J.; and Klement, U. (2012). Characterization of the surface integrity induced by hard turning of bainitic and martensitic AISI 52100 steel. *Procedia CIRP*, 1, 494-499.
19. Hosseini, S.B.; Beno, T.; Klement, U.; Kaminski, J.; and Ryttberg, K. (2014). Cutting temperatures during hard turning - Measurements and effects on white layer formation in AISI 52100. *Journal of Materials Processing Technology*, 214(6), 1293-1300.

20. Bapat, P.S.; Dhikale, P.D.; Shinde, S.M.; Kulkarni, A.P.; and Chinchanikar, S.S. (2015). A numerical model to obtain temperature distribution during hard turning of AISI 52100 steel. *Materialstoday: Proceedings*, 2(4), 1907-1914.
21. Dong, D.Y.; Choi, Y.G.; Kim, H.G.; and Hsiac, A. (1996). Study of the correlation between surface roughness and cutting vibrations to develop an on-line roughness measuring technique in hard turning. *International Journal of Machine Tools and Manufacture*, 36(4), 453-464.
22. Kassab, S.Y.; and Khoshnaw, Y.K. (2007). The effect of cutting tool vibration on surface roughness of workpiece in dry turning operation. *Engineering & Technology*, 25(7), 879- 889.
23. Upadhyay, V.; Jain, P.K.; and Mehta, N.K. (2013). In-process prediction of surface roughness in turning of Ti-6Al-4V alloy using cutting parameters and vibration signals. *Measurement*, 46(1), 154-160.
24. Sahoo, P.; Pratap, A.; and Bandyopadhyay, A. (2017). Modeling and optimization of surface roughness and tool vibration in CNC turning of aluminum alloy using hybrid RSM-WPCA methodology. *International Journal of Industrial Engineering Computations*, 8(3), 385-398.
25. Manivel, D.; and Gandhinathan, R. (2017). Prediction of cutting tool vibration in hard turning using response surface methodology. *International Journal of Advanced Engineering Technology*, 8(1), 1-5.
26. Hessainia, Z.; Belbah, A.A.; Yallese, M.A.; Mabrouki, T.; and Rigal, J.F. (2013). On the prediction of surface roughness in the hard turning based on cutting parameters and tool vibrations. *Measurement*, 46(5), 1671-1681.
27. Izelu, C.O.; Eze, S.C.; and Samuel, O.D. (2016). Modeling and optimization of surface roughness and machining induced vibration in 41cr4 alloy structural steel turning operation using design of experiment. *International Journal of Engineering and Science*, 5(7), 34-44.
28. Plaza, E.G.; and NúñezLópez, P.J. (2017). Surface roughness monitoring by singular spectrum analysis of vibration signals. *Mechanical Systems and Signal Processing*, 84(A), 516-530.
29. Che Sidik, N.A.; Samion, S.; Ghaderian, J.; and Afiq, M.N. (2017). Recent progress on the application of nanofluids in minimum quantity lubrication machining: a review. *International Journal of Heat and Mass Transfer*, 108(A), 79-89.
30. De Godoy, V.A.A; and Diniz, A.E. (2011). Turning of interrupted and continuous hardened steel surfaces using ceramic and CBN cutting tools. *Journal of Materials Processing Technology*, 211(6), 1014-1025.
31. Shihab, S.K.; Khan, Z.A.; Aas, M.; and Siddiquee, A.N. (2014). A review of turning of hard steels used in bearing and automotive applications. *Production & Manufacturing Research*, 2(1), 24-49.
32. Chinchanikar, S.; and Choudhury, S.K. (2015). Machining of hardened steel-experimental investigations, performance modeling and cooling techniques: a review. *International Journal of Machine Tools & Manufacture*, 89, 95-109.
33. Das, S.R.; Mohapatra, D.K.; and Routray, P.C. (2015). Parametric effects and optimization of machining parameters in hard turning: a literature review. *International Journal for Research in Applied Science & Engineering Technology*, 3(2), 7-13.

34. Govindan, P.; and Vipindas, M.P. (2014). Surface quality optimization in turning operations using Taguchi method - a review. *International journal of mechanical Engineering and robotics research*, 3(1), 89-118.
35. Varaprasad, Bh.; Srinivasa, Ra.Ch.; and Vinay, P.V. (2014). Effect of machining parameters on tool wear in hard turning of AISI D3 steel. *Procedia Engineering*, 97, 338-245.
36. Dawson, Ty.G.; and Kurfess, T.R. (2001). Tool life, wear rates, and surface quality in hard turning. *Woodruff School of Mechanical Engineering*, Georgia Institute of Technology, Atlanta, Georgia.
37. Fnides, B.; Boutabba, S.; Fnides, M.; Aouici, H.; and Yallese, M.A. (2013). Tool life evaluation of cutting materials in hard turning of AISI H11. *Estonian Journal of Engineering*, 19(2), 143-151.
38. De Godoy, V.A.A; and Diniz, A.E. (2011). Turning of interrupted and continuous hardened steel surfaces using ceramic and CBN cutting tools. *Journal of Materials Processing Technology*, 211(6), 1014-1025.
39. Azizi, M.W.; Balhadi, S.; Yallesse, M.A.; Lagred, A.; Bouziane, A.; and Boulanouar, L. (2016). Study of the machinability of hardened 100Cr6 bearing steel with tin coated ceramic inserts. *Third International Conference on Energy, Materials, Applied Energetics and Pollution*, Constantine, Algeria, 172-177.
40. Sobiyi, K.K. (2015). Hard turning of martensitic AISI 440B stainless steel. *PhD Thesis, University of the Witwatersrand*, Johannesburg, South Africa.
41. Bartarya, G.; and Choudhury, S.K. (2012). Effect of cutting parameters on cutting force and surface roughness during finish hard turning AISI 52100 grade steel. *Procedia CIRP*, 1, 651-656.
42. Das, S.R.; Kumar, A.; Dhupal, D.; and Mohapatra, S.K. (2013). Optimization of surface roughness in hard turning of AISI 4340 steel using coated carbide inserts. *International Journal of Information and Computation Technology*, 3(9), 871-880.
43. Awadhesh, P.; Choudhury, S.K.; and Chinchanikar, S. (2014). Machinability assessment through experimental investigation during hard and soft turning of hardened steel. *Procedia Materials Science*, 6, 80-91.
44. Kribes, N.; Hessainia, Z.; and Yallesse, M. A. (2016). Optimization of machining parameters in hard turning by desirability function analysis using response surface methodology. *Design and Modeling of Mechanical Systems*, 2, 73-81.
45. Keblouti, O.; Boulanouar, L.; Azizi, M.W.; and Yallesse, M. A. (2017). Effects of coating material and cutting parameters on the surface roughness and cutting forces in dry turning of AISI 52100 steel. *Structural Engineering and Mechanics*, 61(4), 519-526.